JOURNAL OF OPTOELECTRONICS AND ADVANCED MATERIALS, Vol. 11, No. 7, July 2009, p. 950 - 956

Early stage formation of $CuInS_2$ nanocrystals and microspheres by ambient pressure solution synthesis in glycerol

R. BANICA[a*], T. NYARI[a], P. BARVINSCHI[b], P. NEGREA[c], N. VASZILCSIN[c]
[a]*National Institute for Research and Development in Electrochemistry and Condensed Matter, Str. Plautius Andronescu 1, 300224 Timisoara, Romania*
[b] *West University of Timisoara, Bd. V. Parvan 4, 300223 Timisoara, Romania*
[c]*University "Politehnica" of Timisoara, Piata Victoriei 2, 300006 Timisoara, Romania*

In this work we present a new route for rapid synthesis of $CuInS_2$ nanocrystals and microspheres in solution at low temperature and ambient pressure using EDTA-based complexing agents and anhydrous glycerol as solvent. The synthesis experiments were carried out using an experimental set-up which permits sample extraction during the synthesis. The influence of the complexing agent type and reaction time on the morphology and composition of the final products is studied. Following the evolution of phase formation and growth morphologies with the reaction time, a possible growth mechanism of nanocrystals and microspherical nanocrystalline superstructures is proposed.

(Received June 3, 2009; accepted July 20, 2009)

Keywords: $CuInS_2$, Nanocrystals, Microspheres, Photovoltaics

1. Introduction

$CuInS_2$ is one of the most suitable absorbers for thin film solar cells due to its direct band gap near 1.5 eV, high absorption coefficient ($\alpha \sim 10^5$ cm^{-1}) and high-photoconductivity. The type of conductivity (electronic or hole) of this material depends on the stoichiometry, which can be varied by synthesis [1-5].

Many thin film deposition techniques of this ternary compound have been developed for photovoltaic purposes such as radio frequency (RF) reactive sputtering [6], atomic layer deposition (ALD) [7], spray-pyrolysis [8,9] etc. However, all the fabrication methods that imply discontinuous technological processes are expensive and hardly scalable for industrial manufacturing. Solution synthesis methods are more promising because they are relatively cheap and scalable.

$CuInS_2$ has been deposited by chemical bath deposition (CBD) on glass at ambient temperature using as precursors metal sulphates and Na_2S as sulphide ion source. The phase diagram of the Cu_2S – In_2S_3 system allows the existence besides $CuInS_2$ also of other ternary compounds such as $CuIn_3S_5$ and $CuIn_{11}S_{17}$ [10,11].

Guha et al. [12] prepared $CuInS_2$ by metal precipitation at room temperature in aqueous ammonia solution. Precipitation was followed by heat treatment of the obtained powder for crystallization. Thiourea was used as sulphur precursor.

$CuInS_2$ powder has been obtained at 195^{o}C in ethylene glycol from metal chlorides and thiourea by refluxing for 1 h [13]. The authors consider that the stirring of the solution has a great influence on the quality of the final product. Sulfide ions are formed by thermal decomposition of thiourea in the presence of small amounts of water from the metal salts [13].

Nanocrystals with different morphologies of this material are interesting for nanostructured solar cells [14-16] and photocatalytic applications [17,18]. To study the nanocrystal's shape benefits on the solar cells efficiencies, size and shape controlled nanocrystals must be obtained. Although there are some recent reports on the CuInS2 nanocrystals synthesis with different morphologies [18-24], their shape and size controlled growth is not yet understood.

In this paper we present a novel route for the synthesis of $CuInS_2$ nanocrystals and microspheres in solution at low temperature and ambient pressure using EDTA-based complexing agents. The influence of the complexing agent type and reaction time on the morphology and composition of the final products is studied. Following the evolution of phase formation and growth morphologies with the reaction time, a possible growth mechanism of microspherical nanocrystalline superstructures is proposed.

2. Experimental

The synthesis of $CuInS_2$ in solution at low temperature and ambient pressure was carried out using glycerol as solvent and EDTA-based complexing agents.

2.1 Materials

All reagents are p.a. quality and were used as purchased, without further purification. Two types of precursor solutions have been used (denoted "solution 1" and "solution 2"), as follows:

Solution 1

1. 2M HCl and 0.2 mol L^{-1} $C_{10}H_{14}N_2Na_2O_8 \cdot 2H_2O$ (Na_2EDTA) aqueous solution is prepared. This solution is kept in the dark at room temperature for 24 h, then sonicated for 1 min. The resulting opalescent solution is kept again in the dark for 48 h, then the precipitate is filtered, washed with distilled water and dried 6 h at 120ºC. A white powder is obtained, denoted by "P".

2. 1.8140 g $InCl_3 \cdot 4H_2O$ (97%), 0.6123 g CuCl (97%), 3.2 g powder "P" are mixed with 80 mL anhydrous glycerine under magnetic stirring and sonication at 60ºC ± 10ºC until the mixture becomes clear. 1.8834 g thiourea (Tu) (100% exces) and glycerol are added to obtain a 0.05 mol L^{-1} Cu^+ solution. The total volume of the solution is 120 mL and the Cu:In:S molar ratio in the precursor solution is 1:1:4.

Solution 2

Solution 2 is prepared similarly as solution 1 except that powder "P" is replaced by 4.9136 g C_{10} H_{14} $N_2Na_2O_8$ $2H_2O$. The Cu:In:S: Na_2EDTA molar ratio in the precursor solution is kept at 1:1:4:2.2.

2.2 Experimental set-up

The synthesis experiments were carried out using a home-made experimental set-up which permits sample extraction during the synthesis (Fig. 1). The reaction vessel consists of a Teflon autoclave with inner diameter 50 mm and thin walls (1 mm), provided with a thin aluminum housing. The glass stirrer is not in contact with the walls of the autoclave, so that it enables careful stirring of the mixture during the reaction without the risk to damage the freshly formed particles. A slight pressure of argon (5.6 Linde gas) is used to ensure inert atmosphere in the autoclave.

When sample is extracted from the autoclave, a slight vacuum is created in the separatory funnel and consequently the sample is "absorbed" within the argon flow glass tube, open at 1 cm from the bottom of the autoclave, in the funnel. The separatory funnel contains 60 mL ethanol 96% at 0-5ºC, which enables rapid cooling of the sample below 70ºC.

After a given volume of sample was extracted (usually 15-17 mL), the pressure in the separatory funnel is increased and argon continues to flow in the autoclave. Meanwhile, the sample is evacuated from the funnel, the funnel is washed and filled again with ethanol to be prepared for a new sample extraction.

2.3 Procedures

The as-prepared precursor solution (solution 1 or solution 2, respectively) was introduced in the Teflon autoclave. The autoclave was heated by a rate of 4.5 ± 0.3ºC min^{-1} to the reaction temperature (210 ºC). During the reaction, the stirrer was rotated at 180 rpm.

When the reaction temperature was reached, samples were extracted after each 15 minutes and introduced in ethanol (96%). The precipitates were filtered, washed with ethanol and water and dried in air

.

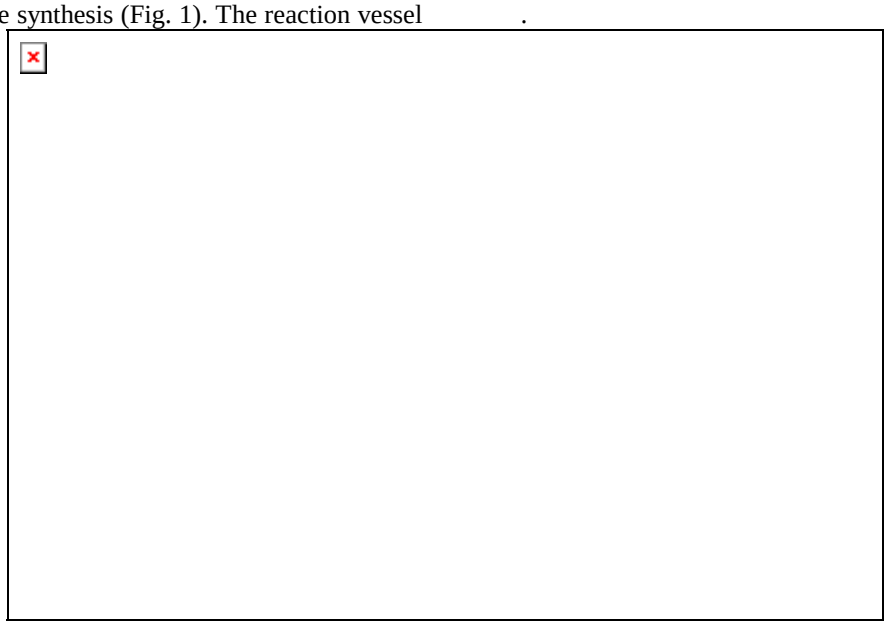

Fig. 1. Schematic representation of the synthesis experimental set-up

2.4 Characterization

The as obtained products were characterized by XRD, SEM/EDAX, AAS and UV-Vis-NIR spectroscopy.

The XRD patterns of powder samples were recorded at room temperature on a BRUKER D8 ADVANCE X-ray diffractometer using Cu Kα radiation (λ = 1.54184 Å, Ni filter) in a θ : 2θ configuration. The peaks of the XRD

patterns were identified using the PDF-4+ Database of JCPDS.

Morphology of the samples and local elemental composition was determined by scanning electron microscopy and energy dispersive X-ray spectroscopy (FEI Inspect S with EDAX).

The global Cu:In ratio in the powders was determined by atomic absorption spectroscopy on samples prepared by digestion of the powders. VARIAN SpectrAA 110 type spectrometer was used with acetylene as fuel, air as oxidizing agent and etalons prepared in the laboratory for calibration. For quantitative determination of Cu and In content, the characteristic lines at 324.8 nm and 303.9 nm, respectively, were used.

The band gap energies have been calculated from the Kubelka-Munk functions obtained from the UV-Vis-NIR diffuse reflection spectra of the powders (Lambda 950 Perkin Elmer, integrating sphere).

3. Results and discussion

Concerning the powder "P" obtained as mentioned above, the XRD pattern show the presence of H_4EDTA crystalline phase in the sample. On the other hand, elemental analysis by EDAX evidenced the presence of chlorine in the powder, due to the ethylenediaminetetraacetic acid chlorohydrates. When powder "P" is prepared at pH<2, penta and hexaprotonated species of the ligand are formed, in which the chloride ion is counterion [25,26].

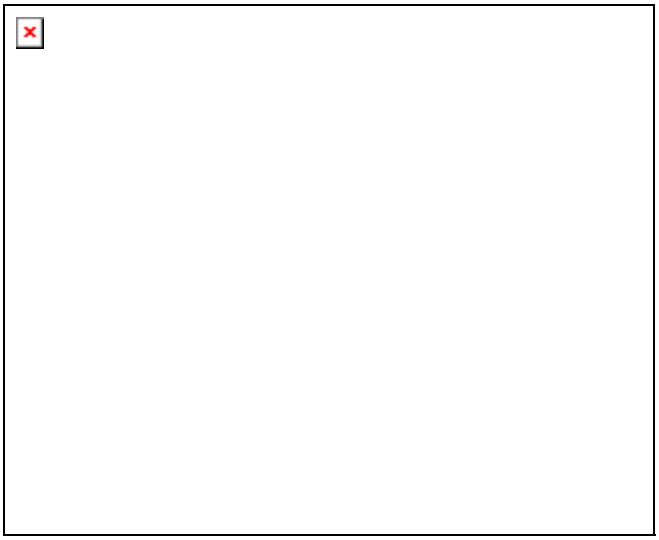

Fig.2. XRD patterns of the samples obtained in solution 1, extracted at 15; 30; 45; 75 minutes after the temperature reached the working value

The XRD patterns for the samples extracted after different reaction times in case of using precursor solution 1 are presented in figure 2. One can observe that the chalcopyrite-type $CuInS_2$ (JCPDS card No. 85-1575) is present as the main phase in the as obtained powder samples, even after very short reaction times (15 min.). At about $2\theta = 26.3^o$ an unidenfied peak denoted "X" is found, which may correspond to an another phase in the $Cu_xIn_yS_z$ system. This peak appears particularly when $CuInS_2$ is deposited by spray pyrolysis from indium rich solutions or at low support temperatures (below 320ºC) [8,27]. This peak can be observed also in the XRD patterns of ref. [13], but it is not mentioned. In this case, the ternary compound was synthesized in ethylene glycol at 195 ºC. In case of solution 1, no significant variation in the XRD pattern is observed for the samples extracted at different reaction times.

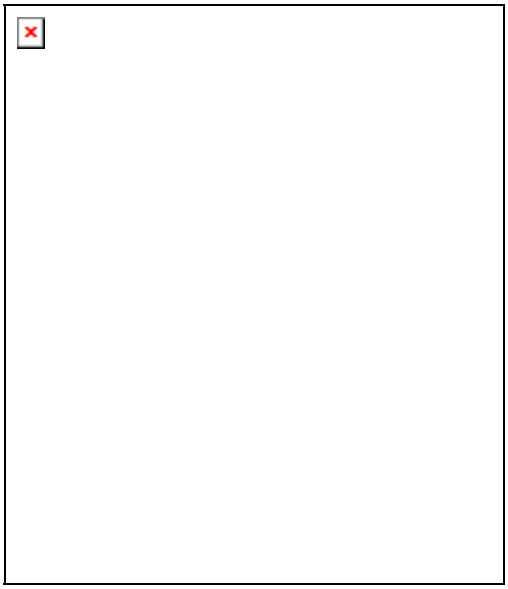

Fig. 3 XRD patterns of the samples obtained in solution 2, extracted at 15; 30; 45; 75 minutes after the temperature reached the working value

In the case of powders obtained using precursor solution 2, from the XRD patterns (figure 3) one can observe that for short reaction times (15 minutes) the $Cu_{1.97}S$ binary is present, which decomposes in time and the formation of $CuInS_2$ takes place. After 75 minutes of reaction, the copper binary is no more present by its characteristic peaks in the XRD pattern. Besides the peaks corresponding to $CuInS_2$ (chalcopyrite), there are two unidentified maxima (denoted X and Y in figure 3) whose intensity is decreasing with the reaction time. According to very recently published results [28-30], these peaks might be attributed to the newly discovered wurtzite metastable polymorph of $CuInS_2$.

Scanning electron microscopy investigations revealed that in the case of precursor solution 1 spherical superstructures with diameters of 1-3 microns with relatively low size distribution are formed (figure 4, A and B). The surface morphology of the spheres is similar to that obtained in ref. [13], although no spheres were obtained in that work.

By contrary, in case of precursor solution 2, nanocrystals resulted without spherical superstructuring. The dimensions of the nanocrystals, determined from electron microscopy images, vary from 80 nm for 15

minutes reaction time (Fig. 4, C) up to about 200 nm after 75 minutes of reaction (Fig. 4, D).

The EDAX investigations indicated that no Cl or Na are present as impurities in the products for both types of precursors (solution 1 and solution 2, respectively).

By a more careful examination of the SEM images of samples obtained in solution 1 one can observe that the microspherical particles have a core-shell structure (figure 4, B), with a relatively smooth core and very rough shell, composed of myriad nanoflakes which seem to originate from the core. To study in more detail these structures, selective dissolution experiments were done, as described below.

In the CIGS-based thin film solar cells fabrication, it is a good practice to remove the copper-rich layer formed on the surface of the CIGS absorber by selective etching the copper-rich compounds with aqueous KCN solution [2,3,31,32]. Usually, KCN etching results in a Cu-poor surface, with the formation of amorphous $In(OH)_xS_y$ or even $In(OH)_3$ on it [4]. With this fact in mind, we made the following experiment.

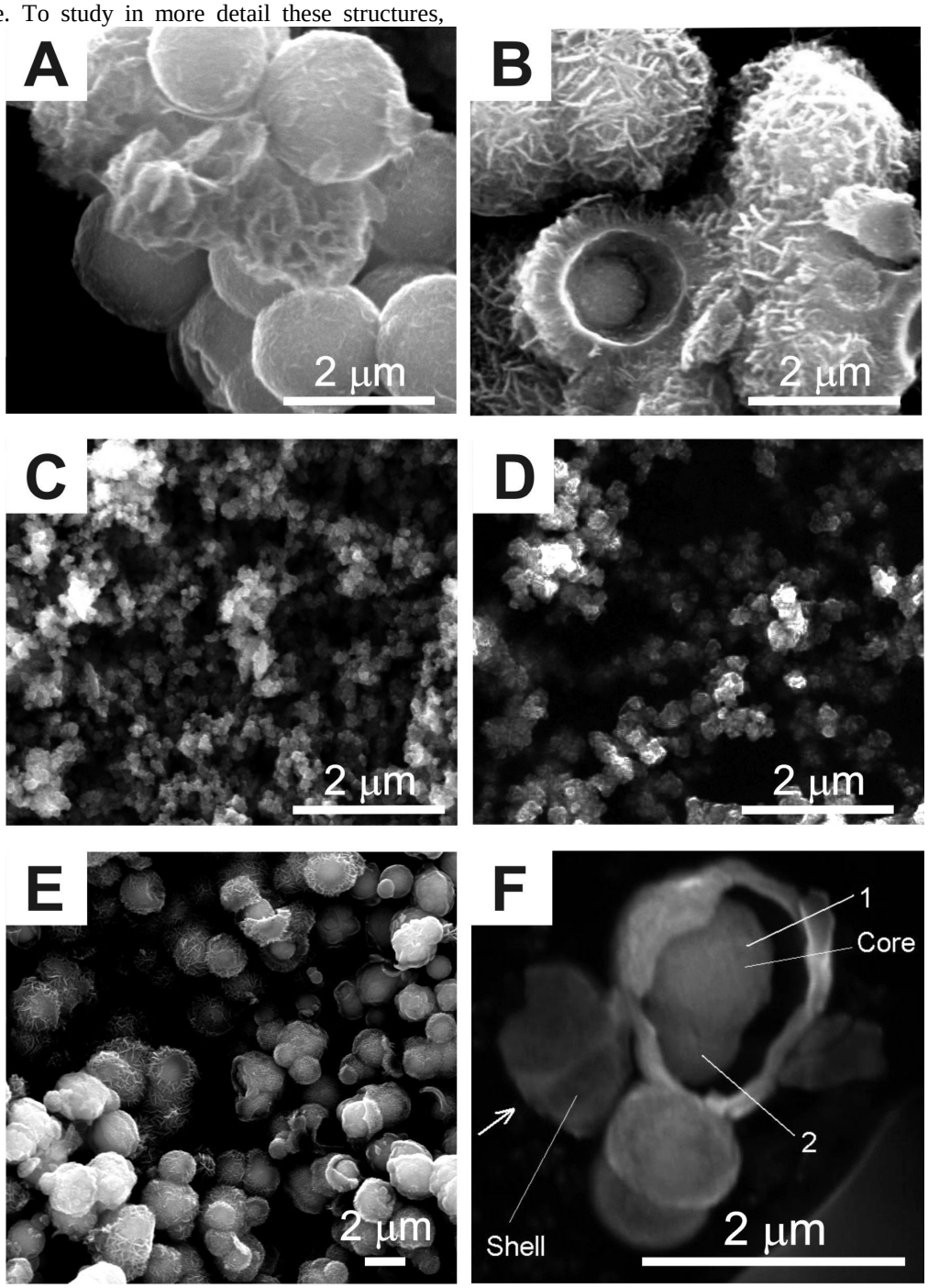

Fig. 4 SEM images of: (A) powders obtained in solution 1 after 30 min. reaction time; (B) powders obtained in solution 1 after 45 min. reaction time; (C) powders obtained in solution 2 after 15 min. reaction time; (D) powders obtained in solution 2 after 75 min. reaction time; (E) sample "D" and (F) sample "D".*

A small quantity of powder from a sample extracted after 75 minutes (solution 1), denoted "sample D", was slightly ground in an agate mortar to break up some spheres, then 150 mg from this sample was subjected to sonication for 20 minutes in a 10% KCN and 1% NaOH aqueous solution at room temperature. After that, the powder was filtered off, washed with distilled water many times and dried at 80°C on the filter paper. The as obtained powder, denoted "sample D*", was then investigated by XRD, SEM and AAS. A quantity of 78 mg of sample D* was obtained, which represents 52% of the initial mass of sample D subjected to etching. The atomic ratio Cu:In in sample D* determined by AAS was 1:1.8, indicating a strong copper depletion. This very low Cu:In ratio in the etched sample by comparison to that before etching (2.18:1, see figure 5, solution 1) might be due to the very high surface area of the ternary semiconductor whose stoichiometry is changed by etching.

In a SEM image of sample D* (figure 4, F) one can observe that an empty area appears between the core and the shell after etching, suggesting a shrinkage of the core, which may be attributed to the preferential dissolution of the core relative to the shell. This might be explained by a more copper rich composition of the core relative to the shell or by a similar composition of the core and shell but smaller particles inside the sphere than outside.

In the case of alkaline aqueous electrolyte solutions, the EDTA ligand decomposes at 175°C with the formation of the relatively stable couple of N-(2-hydroxyethyl) iminodiacetic acid (HEIDA) and iminodiacetic acid (IDA) [33] by the reaction:

$$EDTA + H_2O \rightarrow HEIDA + IDA \qquad [33]$$

The half-life of the ligand concentration is 4.5 h at the above mentioned temperature and pH = 9.4. Martel et al. found by NMR studies that the EDTA ligand decomposes in a first step at 200 °C and pH = 11.4 by C-N bond cleavage, resulting HEIDA and IDA. Its half-life in these conditions is $t_{1/2}$ = 0.5h [34]. At very low concentrations (500 ppm), the indium complex with EDTA is very stable (more than 16 days). At higher temperatures (240°C), this complex decomposes more rapidly, and its concentration is almost zero after two days [35]. No data are available in the literature concerning the indium-EDTA complex stability in glycerol at temperatures above 200°C.

Based on the obtained experimental data (see also below), the following growth mechanisms are proposed corresponding to the synthesis using precursor solution 1 and 2, respectively.

3.1 Precursor solution 1

As the temperature rises, in a first step thermal decomposition of thiourea occurs and chalcogenide nanoparticles are formed which are very rich in copper and poor in indium.

These nanoparticles agglomerate in spherical structures, which sometimes stick together (see for instance 1 and 2 in figure 4, F), giving rise to bigger conglomerates. Supposing that the ligand in the InEDTA complex decomposes in glycerol in the same temperature range as in aqueous ligand solutions, after some time In^{3+} ions will be liberated in solution due to the hexadentate ligand decomposition, with the possible formation of In_2S_3 or of the ternary compound directly. This rise in the free In^{3+} concentration in the solution leads to the beginning of $CuInS_2$ growth as shell on the existing spherical conglomerate cores. With increasing reaction time, the shells are thickened and the copper diffusion out of the core is more difficult, which inhibit the ternary compound formation.

The proposed reactions, taking into account also the small amounts of water present in the system due to hydration water of the metal salts [13], are:

$$OH^- + CS(NH_2)_2 \rightarrow SH^- + NH_4^+ + CNO^- \qquad [36]$$

$$Cu(H_x)EDTA^{(3-x)-} \leftrightarrow Cu^+ + H_xEDTA^{(4-x)-}$$

$$2Cu^+ + S^{2-} \leftrightarrow Cu_2S$$

$$In(H_x)EDTA^{(1-x)-} \leftrightarrow In^{3+} + H_xEDTA^{(4-x)-}$$

$$H_xEDTA^{(4-x)-} \rightarrow \text{decomposition products}$$

$$2In^{3+} + Cu_2S + 3S^{2-} \rightarrow 2\ CuInS_2$$

The atomic ratio Cu:In in the sample extracted after 75 min. (figure 5, solution 1) is 2.18:1, so we can suppose that a considerable proportion of the initial indium introduced in the reaction is at this moment still in the solution incorporated in soluble complexes.

3.2 Precursor solution 2

When precursor solution 2 is used for the synthesis, at low reaction times the product is much more copper-rich than in the solution 1 case (figure 5, solution 2), which is in concordance with the XRD pattern which show a mixture of $CuInS_2$-$Cu_{2-x}S$ phases.

The lower acidity in this case increases the chemical stability of the formed sulphides. At longer reaction times, copper sulphide dissolves and simultaneously indium complex decomposes, having as a result the formation of $CuInS_2$ nanoparticles. The EDTA decomposition products are also ligands. They increase the solubility of the binaries compared to the pure solvent and consequently the ternary formation is accelerated.

Due to the high complexity of the processes involved, further research is needed for a deeper understanding of the ternary compound formation mechanism in this electrolyte solution.

The band gap energies have been calculated from the Kubelka-Munk functions obtained from the UV-Vis-NIR diffuse reflection spectra. By plotting the $[(K\text{-}M)\bullet E]^2$ versus energy (E), the band gap of a powder sample can be extracted [37]. In figure 6 such a plot is presented for the case of sample D*.

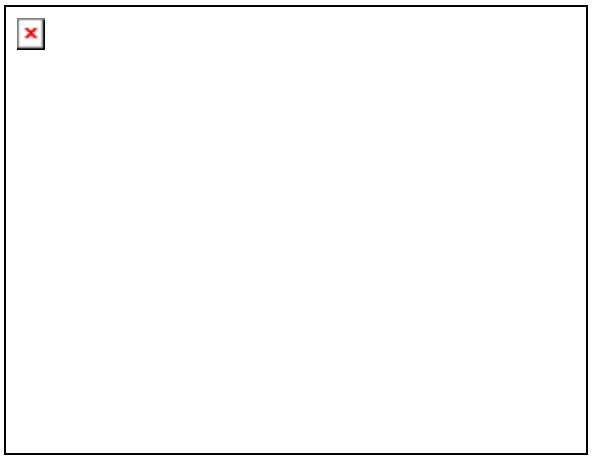

Fig.5 Cu:In atomic ratio evolution with time for samples obtained in solution 1 and solution 2

The band gap energy value cannot be uniquely determined for the as obtained powder (sample D), probably due to the presence of other phase(s) besides $CuInS_2$ and of more defect structure. After KCN etching, the disordered and highly defect phases are dissolved and the absorption edge is steeper. The determined band gap energy value for the sample D* is 1.53 eV, which is close to the 1.5 eV value corresponding to single crystal $CuInS_2$ at room temperature [5].

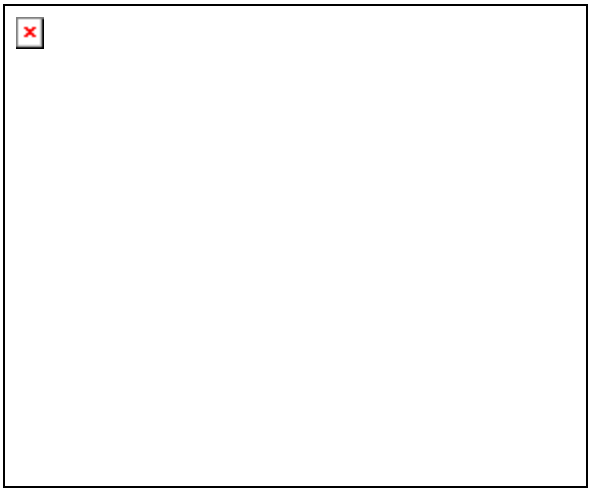

Fig. 6 $[(K-M)\bullet E]^2 = f(E)$ plot for sample D.*

4. Conclusions

A new route to the synthesis of $CuInS_2$ nanocrystals and microspheres in solution at low temperature and ambient pressure using EDTA-based complexing agents and anhydrous glycerol as solvent is presented.

The growth morphology of the particles and the Cu:In ratio in the products depends on the complexing agent type and the reaction time. Using precursor solution 1 core-shell type spherical superstructures were obtained. After their etching in aqueous KCN solution, the core is much more dissolved than the shell. Therefore, the core is more Cu-rich than the shell and serves as nucleation support for the growth of the later. When precursor solution 2 is used for the synthesis, the final product is composed from nanocrystals with dimensions in the range 80-200 nm.

Acknowledgements

This work was financially supported by PN II Research Program 4 of the Romanian Ministry of Education, Research and Innovation, Contract no. 22-124/2008, H2SOLAR project.

References

[1] I. Konovalov, Thin Solid Films **451–452**, 413 (2004).
[2] M. Nanu, J. Schoonman, A. Goossens, Thin Solid Films **451–452**, 193 (2004).
[3] J. Verschraegen, M. Burgelman, J. Penndorf, Thin Solid Films **451–452,** 179 (2004).
[4] H. J. Lewerenz, Solar Energy Materials & Solar Cells **83,** 395 (2004).
[5] J. L. Shay, J. H. Wernick, Ternary Chalcopyrite Semiconductors: Growth, Electronic Properties and Applications, Pergamon Press, New York, 1975.
[6] Y. B. He, A. Krost, J. Bläsing, W. Kriegseis, A. Polity, B.K. Meyer, C. Kisielowski, Thin Solid Films **451–452,** 229 (2004).
[7] M. Nanu, L. Reijnen, B. Meester, A. Goossens, J. Schoonman, Thin Solid Films **431-432**, 492 (2003).
[8] O. Kijatkina, M. Krunksa, A. Mere, B. Mahrov, L. Dloczik, Thin Solid Films, **431-432** 105 (2003).
[9] A. Mere, O. Kijatkina, H. Rebane, J. Krustok, M. Krunks, Journal of Physics and Chemistry of Solids **64,** 2025 (2003).
[10] H. M. Pathan, C.D. Lokhande, Applied Surface Science **239**, 11 (2004).
[11] K. Müller, R. Scheer, Y. Burkov, D. Schmeißer, Thin Solid Films **451–452,** 120 (2004).
[12] P. Guha, D. Das, A. B. Maity, D. Ganguli, S. Chaudhuri, Solar Energy Materials & Solar Cells **80,** 115 (2003).
[13] G. Shen, D. Chen, K. Tang, Z. Fang, J. Sheng, Y. Qian, Journal of Crystal Growth **254,** 75 (2003).
[14] E. Arici, N.S. Sariciftci, D. Meissner, Advanced Functional Materials **15,** 165 (2003).
[15] M. Nanu, J. Schoonman, A. Goossens, Nano Letters **5**, 1716 (2005).
[16] M. Nanu, J. Schoonman, A. Goossens, Advanced Functional Materials **15**, 95 (2005).
[17] F.A. Thiel, Journal of The Electrochemical Society **129,** 1570 (1982).
[18] L. Zheng, Y. Xu, Y. Song, C. Wu, M. Zhang, Y. Xie, Inorganic Chemistry **48**, 4003 (2009).
[19] T. Nyari, P. Barvinschi, R. Baies, P. Vlazan, F. Barvinschi, I. Dékány, Journal of Crystal Growth **275,** 2383 (2005).
[20] M. Rajamathi, R. Seshadri, Current Opinion in Solid State & Materials Science **6**, 337 (2002).

[21] H. Hu, B. Yang, X. Liu, R. Zhang, Y, Qian, Inorganic Chemistry Communications **7,** 563 (2004).
[22] S. Peng, J. Liang, L. Zhang, Y. Shi, J. Chen, Journal of Crystal Growth **305,** 99 (2007).
[23] X. Gou, F. Cheng, Y. Shi, L. Zhang, S. Peng, J. Chen, P. Shen, Journal of the American Chemical Society **128**, 7222 (2006).
[24] X. Cao, L. Gu, L. Zhuge, W. Qian, C. Zhao, X. Lan, W. Sheng, D. Yao, Colloids and Surfaces A: Physicochem. Eng. Aspects **297,** 183 (2007).
[25] G. N. Kaluderović, S. Gómez-Ruiz, H. Schmidt , D. Steinborn, Acta Crystallographica E, **63**, o3491 (2007).
[26] Z. Szakács, S. Béni, B. Noszál, Talanta **74** 666 (2008).
[27] J. D. Harris, K. K. Banger, D. A. Scheiman, M. A. Smith, M. H. -C. Jin, A. F. Hepp, Materials Science and Engineering B **98,** 150 (2003).
[28] Y. Qi, Q. Liu, K. Tang, Z. Liang, Z. Ren, X. Liu, The Journal of Physical Chemistry C **113**, 3939 (2009).
[29] B. Koo, R.N. Patel, B.A. Korgel, Chemistry of Materials **21,** 1962 (2009).
[30] S. T. Connor, C. M. Hsu, B. D. Weil, S. Aloni, Y. Cui, Journal of the American Chemical Society **131,** 4962 (2009).
[31] A. Antony, A.S. Asha, R. Yoosuf, R. Manoj, M. K. Jayaraj, Solar Energy Materials & Solar Cells **81**, 407 (2004).
[32] R. P. Wijesundera, W. Siripala, Solar Energy Materials & Solar Cells **81,** 147 (2004).
[33] R. J. Motekaitis, X. B. Cox, P. Taylor, A. E. Martell, B. Miles, T.J. Tvedt, Canadian Journal of Chemistry **60,** 1207 (1982).
[34] A. E. Martell, R. J. Motekaitis, A. R. Fried, J. S. Wilson, D.T. MacMillan, Canadian Journal of Chemistry **53,** 3471 (1975).
[35] C. V. Chrysikopoulos, P. Kruger, Chelated Indium Activable Tracers for Geothermal Reservoirs, Stanford Geothermal Program Interdisciplinary Research in Engineering and Earth Sciences, Stanford, California, June 1986.
[36] W. H. R. Shaw, D. G. Walker, Journal of the American Chemical Society **78**, 5769 (1956).
[37] A. E. Morales, E.S. Mora, U. Pal, Revista Mexicana Física S **53,** 18 (2007).

*Corresponding authors: benny_van_li@yahoo.com